Available online at www.sciencedirect.com
ScienceDirect
Geochimica et Cosmochimica Acta 70 (2006) 6153–6167
Geochimica
www.elsevier.com/locate/gca

Compositional trends among IID irons; their possible formation from the P-rich lower magma in a two-layer core

John T. Wasson *, Heinz Huber

Institute of Geophysics and Planetary Physics, University of California, Los Angeles, CA 90095-1567, USA

Received 4 November 2005; accepted in revised form 18 January 2006

Paper dedicated to the memory of Larry Haskin

Abstract

Group IID is the fifth largest group of iron meteorites and the fourth largest magmatic group (i.e., that formed by fractional crystallization). We report neutron-activation data for 19 (of 21 known) IID irons. These confirm earlier studies showing that the group has a relatively limited range in Ir concentrations, a factor of 5. This limited range is not mainly due to incomplete sampling, Instead, it seems to indicate low solid/liquid distribution coefficients reflecting very low S contents of the parental magma, the same explanation responsible for the limited range in group IVA. Despite this similarity, these two groups have very different volatile patterns. Group IVA has very low abundances of the volatile elements Ga, Sb and Ge whereas in group IID Ga and Sb abundances are the highest known in a magmatic group of iron meteorites and Ge abundances are the second highest (after group IIAB). Group IID appears to be the only large magmatic group having high volatile abundances but low S. In the volatile-depleted groups IVA and IVB it is plausible that S was lost as a volatile from a chondritic precursor material. Because group IID seems to have experienced minimal loss of volatiles, we suggest that S was lost as an early melt having a composition near that of the Fe–FeS eutectic (~315 mg/g S). When temperatures had risen 400–500 K higher P-rich melts formed, became gravitationally unstable, and drained through the first melt to form an inner core that was parental to the IID irons. As discussed by [Kracher, A., Wasson, J.T., 1982. The role of S in the evolution of the parental cores of the iron meteorites. *Geochim. Cosmochim. Acta* **46**, 2419–2426], it is plausible that a metal-rich inner core and a S-rich outer core could coexist metastably because stratification near the interface permitted only diffusional mixing. The initial liquidus temperature of the inner, P-rich core is estimated to have been ~1740 K; after >60% crystallization the increase in P and the decrease in temperature may have permitted immiscibility with the S-rich outer core. We have not recognized samples of the outer core.

1. Introduction

It was previously known that S contents were low in the two volatile-depleted magmatic groups IVA and IVB. Group IID, with 21 members, is the fifth largest group of iron meteorites and the fourth largest magmatic group. It also has a low S content but has high contents of other volatiles. In this paper we explore how this surprising juxtaposition might have been created.

The compositional and structural properties of group IID were discussed by Wasson (1969), Buchwald (1975) and Scott and Wasson (1975). We here present INAA (instrumental-neutron-activation-analysis) data for 19 IID irons; the only data previously published were for Vicenice (Wasson et al., 1989), thus this is the first comprehensive study of the group using this technique.

Wasson (1999) noted that the IIIAB Ir-Au and Ir-As trends could be explained by a combination of fractional crystallization and equilibrium melt trapping. Wasson and Richardson (2001) used the same approach to model

* Corresponding author. Also: Department of Earth and Space Sciences and Department of Chemistry and Biochemistry, University of California, Los Angeles, USA. Fax: +1 310 206 3051.
E-mail address: jtwasson@ucla.edu (J.T. Wasson).

0016-7037/$ - see front matter © 2006 Elsevier Inc. All rights reserved.
doi:10.1016/j.gca.2006.01.032

the compositions of IVA irons. In this paper we apply this model approach to evaluate the formation of the IID irons.

In a metallic magma the solid/liquid distribution coefficient D for S is very small; in our studies we assume the D_S value to be 0.005. As a result, S remains almost quantitatively in the melt during the crystallization of metallic magmas. Because so little S enters into the crystallizing metal, exsolution of S at low temperatures is negligible. Thus the FeS nodules that are common in iron meteorites reflect the presence of trapped melt.

During the past three decades solid/liquid distribution coefficients for metallic systems have received considerable study, particularly in the Drake lab at the University of Arizona. Reviews have been published by Jones and Drake (1983), Jones and Malvin (1990) and Chabot and Jones (2003). Most D values are strongly dependent upon the nonmetal (S, P, C) concentrations in the melt.

For the siderophile elements one can estimate the initial composition of the molten core by constructing fractionation models that account for the general elemental trends, generally plotted as log element-log Ni or log element-log Au diagrams (e.g., Wasson and Richardson, 2001). The initial composition of the melt is the mean composition of the magma.

It is much more difficult to estimate the concentration of nonmetals in the core. Because S is generally the most abundant nonmetal, most effort has been spent on attempting to assess its concentration. Esbensen et al. (1982) and Wasson (1999) modeled the large variations in trapped melt observed among the different large masses of the Cape York iron to estimate the S concentration in the IIIAB core. We discuss evidence indicating that the S abundance in IID was quite low, similar to that in the IVA magma.

No silicates have been reported for group IID but it does contain the oxide chromite. This offers the possibility of obtaining a key taxonomic parameter, the O-isotopic composition, that can be used to link the group with known groups of chondrites. No O-isotopic data have been reported to date, perhaps because (as discussed below) the chromites are quite small.

2. Analytical techniques and samples

We currently determine up to 15 elements (14 plus Fe) in metal by instrumental-neutron-activation analysis (INAA) in replicate analyses; data for Fe are used for internal normalization. We recently started to determine Ru routinely; only a few values are reported in this data set. All Ge and (with one exception) Sb data reported here were determined by radiochemical neutron-activation analysis (RNAA). With INAA we can measure Ge at IID levels, but the relative uncertainties are high, roughly ±20% relative, and to avoid mixing such results with precise RNAA data we have chosen to not report these. Our INAA detection limit for Sb is relatively high (about 120 μg/g) and we here report only one value (in Wallapai) determined by this technique as well as three values determined by RNAA.

Most meteorites were analyzed two or three times to improve the precision. The procedures are those given by Wasson et al. (1989) except for two minor changes. The mean sample thickness is now 3.0 instead of 3.2 mm, and we now apply small (generally in the range 0.95–1.05) sample-specific geometric corrections to make the Ni values in the first count agree better with those from the third and fourth counts (which are corrected to make Fe + Ni = 990 mg/g). We then choose a correction factor for the second count that is intermediate between that for the first and the mean corrections in the third and fourth counts. We minimize contamination of our samples by careful preparation and by a brief etching with a dilute mix of HCl and HNO_3 following the irradiation.

Although the INAA data were gathered over almost three decades, significant improvements in the quality were achieved starting in 1986. As a result, some meteorites were restudied and the recent analyses given double weight in the determination of the means. In most meteorites we had previously determined Ni by atomic-absorption spectrophotometry; in these cases the Ni means were calculated treating the previous mean as an additional replicate. We have now recalculated older analytical runs to incorporate these more sophisticated correction procedures. We did not use Filomena as a standard in our oldest runs; instead we irradiated aliquots of standardized solutions, a technique that was less reproducible. In our recalculations we have used newer analyses of some of the irons in these earlier runs to restandardize the data; most of the revisions are smaller than 5% relative.

We estimate relative 95% confidence limits on the listed means to be 1.5–3% for Co, Ni, Ga, Ir and Au, 4–6% for As and (RNAA) Ge, 7–10% for Ru (values >2 μg/g); W (values >0.3 μg/g), Sb (>200 ng/g), Re (>50 ng/g) and Pt (>2 μg/g). Because much of the Cr is in minor phases (mainly chromite), sampling errors result in relative confidence limits on the mean ⩾10%. In addition, there is an Fe interference in the determination of Cr resulting from the $^{54}Fe(n,\alpha)^{51}Cr$ fast-neutron reaction; our somewhat uncertain estimate of the level of interference is 6 μg Cr per gram of Fe (Wasson and Richardson, 2001). Our data were not corrected for this interference.

In runs carried out during the past two decades we used three INAA standards, two of which are IIAB irons, the Filomena specimen of the North Chile shower and a Coahuila specimen off an undetermined mass of this shower. We find Filomena to be a very uniform iron, and thus well suited to be a standard. Only Cr shows moderate scatter (a standard deviation of about 10% relative). Coahuila is slightly more variable in its composition, but is adequately uniform for use as a secondary standard. Our third standard is the NBS steel 809B; the high Mn content of NBS 809B causes it to be too radioactive to include in the first count several hours after the end of an irradiation.

The 19 meteorites listed in Tables 1 and A1 comprise the entire known set of IID irons save Richa (heavily weathered, our RNAA Ir value is 16.5 μg/g Ir) and the

Table 1
Mean concentrations of 15 elements in 19 IID iron meteorites; meteorites arranged in order of increasing Au content

	Cr (μg/g)	Co (mg/g)	Ni (mg/g)	Cu (μg/g)	Ga (μg/g)	Ge (μg/g)	As (μg/g)	Ru (μg/g)	Sb (ng/g)	W (μg/g)	Re (ng/g)	Ir (μg/g)	Pt (μg/g)	Au (μg/g)	P (mg/g)
NEA002[a]	132	6.58	102.2	259	70.6		4.25	20.3		3.01	2150	22.6	22.4	0.556	—
Arltunga[a]	121	6.40	96.6	264	71.7	83.0	4.06	19.8		2.86	2070	20.6	21.6	0.559	2.4
Losttown	46	6.60	96.0	287	71.9	78.0	4.11		93	3.07	2020	20.7	19.3	0.564	2.5
N'Kandhla	68	6.76	96.0	253	71.3	83.3	4.33			3.03	1940	19.6	19.9	0.585	3.0
Cheder	54	6.62	100	267	71.5		4.59	20.0		3.00	1620	17.5	20.2	0.586	—
Bridgewater	202	6.63	99.2	274	74.9	82.0	4.59			2.98	2020	19.7	22.0	0.599	3.5
Alt Bela[b]	82	6.55	100.9	288	73.6	83.9	4.45		85	2.79	1720	15.9		0.618	3.9
St. Augustine	85	6.66	100.5	266	74.7		4.76			3.11	1980	19.4	22.3	0.608	—
Elbogen	53	6.70	99.9	270	74.3	85.9	5.01			2.92	1580	15.9	19.0	0.641	3.0
Mafuta	62	6.71	100.3	264	72.7		5.00			2.92	1390	15.4	19.8	0.645	—
Puquios	48	6.67	99.3	263	76.4	87.9	5.04			4.04	1390	14.3	19.9	0.655	3.5
Carbo	88	6.69	101.7	320	77.1	87.2	5.19			3.44	1420	14.3	22.4	0.671	4.0
Hraschina	77	6.89	103.3	299	77.0	90.7	5.55			2.56	1470	14.6	19.6	0.700	>4
Mount Ouray	86	6.69	98.8	265	73.9	84.4	5.78			3.18	1740	17.8	23.0	0.700	4.0
Brownfield	46	6.73	98.7	279	75.4	85.3	5.33			2.95	1260	12.9	20.1	0.722	—
Vicenice	61	6.75	101.0	279	76.1	87.4	6.66		109	2.91	1170	12.6	16.7	0.762	—
Rodeo	138	6.88	104.8	251	76.5	93.0	8.20			2.46	1070	10.2	15.5	0.947	7.5
Needles	31	7.01	106.9	249	85.6	93.4	11.8			2.19	510	5.37	13.3	1.404	8.5
Wallapai	32	6.91	111.4	241	84.3	99.1	13.5		154	2.07	410	3.99	11.6	1.533	9.0

All data obtained by INAA except Ge and two Sb values (both RNAA) and P (modal analysis by Buchwald, 1975).
This table available in digital form in electronic annex EA.
[a] These two irons are classified as anomalous members of group IID mainly because of their deviant structures; see text for details.
[b] Alt Bela data are of lower quality because the sample was oxidized and the technique was not well developed at the time the analyses were completed.

small (83-g) Antarctic iron MIB 03002 (D'Orazio and Folco (2003) reported an Ir concentration of 11.3 μg/g). The number of well characterized iron meteorites is ca. 740 thus the mean IID abundance among irons is 2.8% (±0.6%).

3. Results

3.1. Compositional data

In Table 1 we list mean INAA data for 14 elements as well as P data from Buchwald (1975). As noted above, we also determine Fe but use it to correct for geometric effects or for the presence of appreciable amounts on nonmetallic inclusions. To facilitate locating meteorites in the diagrams we list the mean compositions of the 19 IID irons in order of increasing Au concentration in Table 1. Individual analyses are listed alphabetically in Table A1 in the Appendix together with the irradiation dates.

Our data are plotted on log element-log Au scatter diagrams in Figs. 1 and 2. Also plotted as a reference cloud are IIIAB data having Au concentrations lower than 1.6 μg/g. Some IIIAB concentration data have been increased by factors indicated on the individual diagrams to make them plot closer to the IID irons (and, by making the slopes appear larger, to make the trends more easily recognized).

It is widely accepted that the main IIIAB trends formed as a result of fractional crystallization. The IID trends are roughly parallel to those in IIIAB on all 10 diagrams, in support of the conclusion that the IID irons also formed by fractional crystallization.

3.2. Petrographic observations

Buchwald (1975) gives detailed structural information regarding 14 IID irons. These include all the 19 irons listed in Table 1 except Cheder, St. Augustine, Mafuta, NEA 002 and Vicenice. Buchwald (1975) described Losttown but mistakenly guessed that it was a IIIAB iron. He also described Richa which was not included in our study because of its high level of corrosion. And, like us, he did not have access to the new Antarctic IID iron MIB 03002.

Two of the IID irons, Arltunga and NEA 002, have anomalous textures suggesting later reheating. All others are medium octahedrites with kamacite bandwidths in the range 0.65–0.85 mm except Needles (0.47 mm) and Wallapai (0.43 mm); the latter, which have the highest Ni contents among IID irons, are fine octahedrites. These bandwidths are roughly similar to those in IIIAB irons having similar Ni contents, leading to the inference that the cooling rates are similar to those in IIIAB.

The two irons with anomalous structures, Arltunga and NEA 002, are at the low-Au, high-Ir extreme of the compositional range. Buchwald (1975) discusses Arltunga in some detail. He describes it as an ataxite with a microscopic Widmanstätten pattern in which the mean thickness of the kamacite lamellae is 5 μm. The schreibersite is also uniformly distributed as 1–5 μm rounded blebs. He concludes that Arltunga records an exceptionally high cooling rate through the $\alpha + \gamma$ field.

The structure of NEA 002 consists of small domains having dimensions of 5–10 mm that show different sheens in reflected light. Each of these domains is filled with a

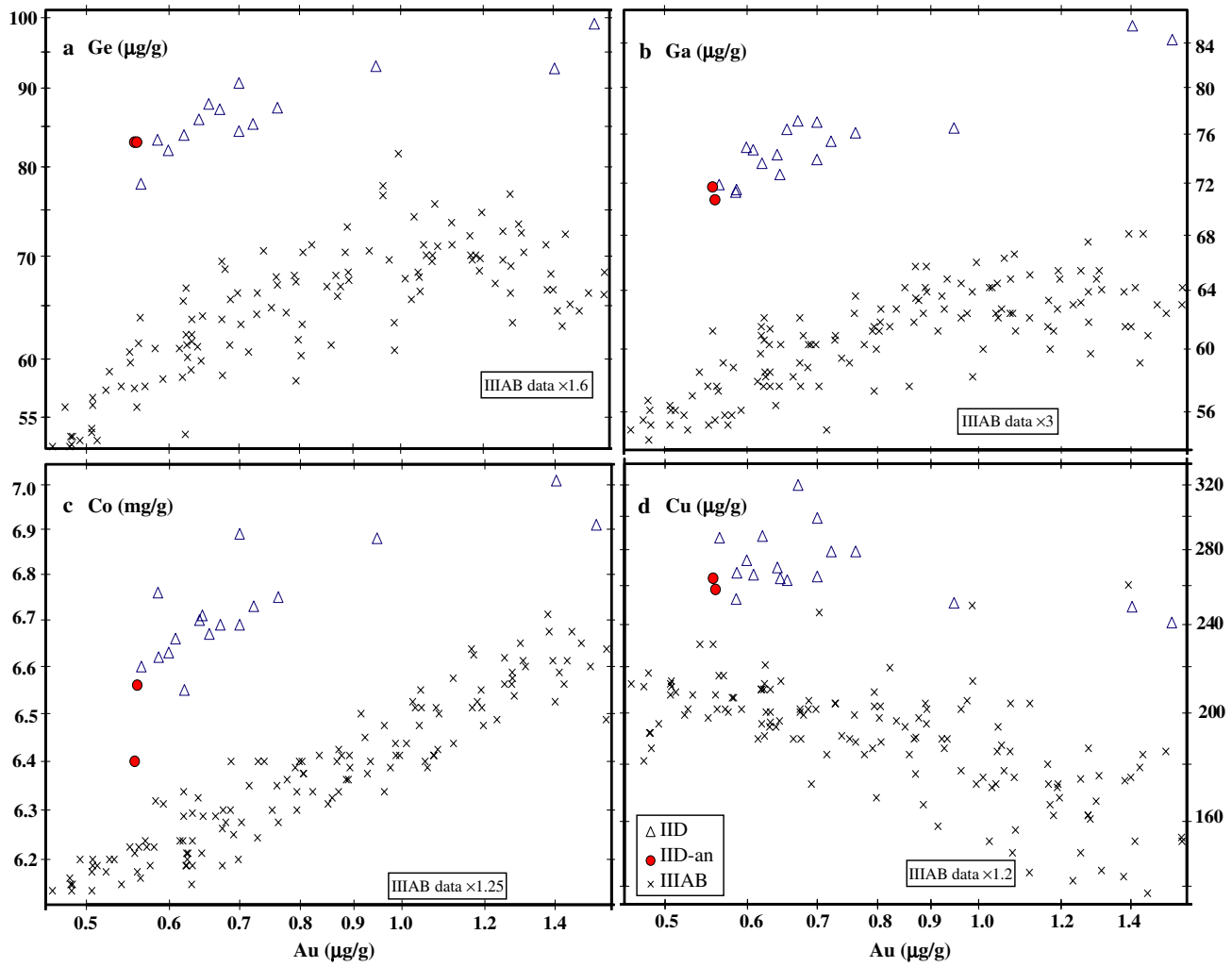

Fig. 1. Log element-log Au diagram showing IID trends for four taxonomic elements that show relatively small ranges within the group: (a) Ge; (b) Ga; (c) Co and (d) Cu. Shown as a background cloud are the IIIAB data having Au contents smaller than 1.6 μg/g.

fine-Widmanstätten pattern of kamacite bandlets, typically in parallel clusters of several bands, each ~0.2 mm wide, appreciably wider than those in Arltunga. No inclusions are identifiable at low magnification. Cracks are present between several of the domains. Because of their exceptional textures we designate Arltunga and NEA 002 anomalous members of IID (IID-an). As discussed in the following section their compositions are essentially normal IID, but at the low-Au, high-Ir extreme.

These observations suggest that, if Arltunga and NEA 002 formed together with the other IID irons, they suffered a reheating event that caused resorption of kamacite followed by cooling in an environment that offered much less thermal insulation than that recorded by the normal members of the group. The probable explanation is that they were heated by impact and that, following this event, the amount of thermal insulation was low, but greater near NEA 002 than that around Arltunga.

As noted by Buchwald (1975), the IID irons have relatively high schreibersite contents but troilite (and thus S) is relatively rare. He reported a S abundance in Arltunga, 0.2 mg/g, that is one of the lowest in an iron meteorite. In most of these irons the largest troilites in a section are about 1 mm across. In his description of Wallapai Buchwald states: "Troilite is conspicuous by its absence. On polished sections totaling 1200 cm^2 the largest troilite crystal was 1 mm across, and inspection of the exterior surface of the two main masses also failed to disclose any pits which could be unequivocally attributed to troilite. It appears that the chemical group IID is characterized by, among other things, its low content of troilite. The little troilite present (in Wallapai) is associated with schreibersite, forming monocrystalline blebs and elongated bodies, often with 15% daubreelite as parallel bars in the troilite." It appears that the only IID iron that shows the presence of (minor amounts of) trapped melt is Carbo, in which Buchwald reports: "Troilite occurs in scattered nodules and in what appears to be pencil-like inclusions. Cross sections are 5–25 mm in size and indicate some uniform flattening." On the surface of Carbo he observed "10 almost parallel cylindrical holes, up to 15 mm in diameter and 70 mm deep (that) may indicate the previous location of troilite-belem-

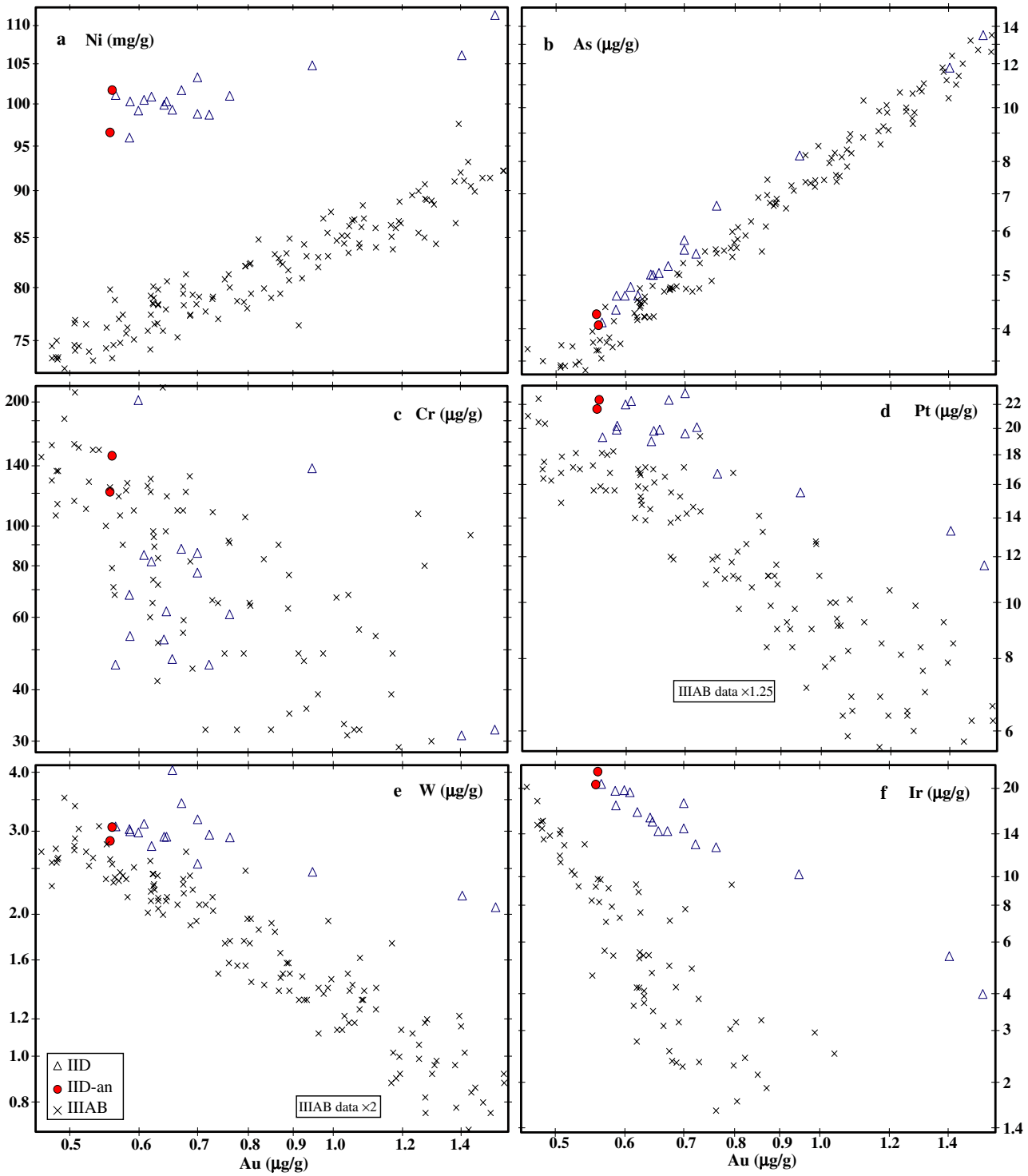

Fig. 2. Log element-log Au diagram showing IID trends for six elements: (a) Ni; (b) As; (c) Cr; (d) Pt; (e) W and (f) Ir. The first two are incompatible and, like Au, are frequently employed as independent variables in iron-meteorite studies. The third, Cr, shows much scatter and is not a true siderophile, occurring mainly as chromite, daubreelite or CrN. The last three elements are compatible, with D_{Ir} being appreciably larger that D_{Pt} and D_W. Again shown as a background cloud are data for IIIAB irons having Au contents smaller than 1.6 μg/g.

nites; compare Cape York, La Caille and Santa Rosa." We will return to the question of trapped melt below.

Buchwald (1975) observed graphite in Elbogen and a carbide, probably haxonite, in the martensitic fields of Carbo. Carbides were present in one out of five plessite fields and described as "carbide roses, 100–800 μ across".

Buchwald reported that chromite ($FeCr_2O_4$) is present in most IID irons, generally associated with schreibersite. As noted above, Cr is also present as daubreelite ($FeCr_2S_4$) exsolution lamellae in FeS. Generally Buchwald (1975) only mentions the one or the other of the two Cr minerals; the exception is Losttown in which he observed "In one

place an 800 × 100 μm chromite crystal has served as nucleus for the growth of a 500 × 200 μm troilite, which later has precipitated a 500 × 30 daubreelite lamellae parallel to and in direct contact with the chromite.'' In Carbo the chromite may reach sizes >1 mm, large enough to permit O-isotopic study.

In Carbo Marvin (1962) observed a small patch of SiO_2-rich glass from which cristobalite had exsolved; the glass was sited in a troilite inclusion.

4. Element-Au trends in group IID; comparison with those in group IIIAB

In Figs. 1 and 2 we illustrate the element-Au trends in IID and show (as a cloud of points) the data from group IIIAB, the largest iron-meteorite group (and also a magmatic group). We used different symbols (filled circles) for the two structurally anomalous members Arltunga and NEA 002; both plot at the low-Au extreme of the IID group.

In Fig. 1 we show element-Au plots for four elements that are important for iron meteorite taxonomy because they show restricted ranges within the groups but much larger ranges among the entire set of iron meteorites. The classic taxonomic elements Ge and Ga (Fig. 1a and b) show trends similar to those in the large set of IIIAB irons, including an apparent decrease in slope with increasing Au content (and increasing degree of crystallization). The Co field (Fig. 1c) shows a very small range in IID (note the label on the *Y* axis) but a clearly defined positive trend having a slope similar to or slightly lower than that in IIIAB. The Cu trend (Fig. 1d) is downward, and the slope is roughly similar to that in IIIAB; in both groups a small fraction of the irons show anomalous concentrations that are generally high. We suspect this reflects the occasional (stochastic) sampling of Cu-rich trapped melt or exsolved Cu metal.

Note that the two IID irons with anomalous textures (filled circles) are compositionally normal on all four diagrams with the exception of the 2% low Co concentration in NEA 002. We do not have a precise Ge concentration for NEA 002.

On Fig. 2 we show element-Au diagrams for two incompatible reference elements (Ni and As), three compatible elements (Pt, W and Ir) and Cr, which shows a negative trend but much scatter. We call Ni, As and Au reference elements because they frequently serve as the independent variables on scatter diagrams. They are well suited for this role because they show ranges much larger than experimental uncertainty for each iron, and because they form linear trends when plotted against one another.

The Ni–Au trends in IID and IIIAB show similar slopes, though slightly lower in IID (Fig. 2a). We chose not to offset the IID and IIIAB data on the As–Au diagram (Fig. 2b) even though this makes it more difficult to resolve the groups; note that, at low Au concentration, the IID irons are all on the upper fringe of the IIIAB cloud, and that the two high-Au IID irons are only slightly inside the IIIAB field. The slopes are thus nearly identical. The two IID-an irons plot along the group trend.

There is much scatter in the Cr–Au data (Fig. 2c). This almost certainly indicates that a large fraction of the Cr is in nonmetallic phases, especially chromite or Cr-rich melt inclusions. There is no resolvable difference between the scatter fields of IID and IIIAB; both the Cr concentrations and the variances are similar. As discussed by various authors (e.g., Wasson and Richardson, 2001), these negative trends are the opposite to those expected based on laboratory studies that yield D_{Cr} values around 0.5 (e.g., Jones and Drake, 1983). To account for the negative trend Wasson et al. (1999) suggested sampling biases resulting from the Cr-bearing phase ($FeCr_2O_4$ or possibly CrN) being finely divided and commonly trapped in the metal of low-Au irons (and thus included in metallic samples) but coarse and avoidable when sampling the high-Au meteorites. Another possibility is that chromite was a liquidus phase, thus causing Cr to behave like a compatible siderophile (Ulff-Møller, 1998a) The sampling interpretation is supported by the presence of massive chromite in the Brenham main-group pallasite whereas the Cr content of the metal is low, ca. 30 μg/g (Wasson et al., 1999).

As discussed in the next section, the inferred Ni-normalized initial Cr abundance of the IID magma is ~100 × lower than chondritic levels. This may indicate that most of the Cr in the chondritic precursor was oxidized (as $FeCr_2O_4$) and thus only a small fraction partitioned into the segregating molten metal. This implies, however, that $FeCr_2O_4$ was a liquidus phase when metal began crystallizing from the IID magma. As noted by Ulff-Møller (1998a) and others, cocrystallization of chromite could help explain the observed negative trends on Cr–Au or Cr–Ni diagrams. Because the chromite density is low (4.8–5.0 g cm^{-3}) it would have risen buoyantly to the top of the inner core, even if attached to a comparable volume of solid metal. We return to this point below.

In both IID and IIIAB the three refractory elements Pt, W and Ir show steeply negative trends on element-Au plots (Figs. 2d–f). For each element the slopes are appreciably lower in IID than in IIIAB; as discussed in the following section, the lower slopes on refractory siderophile vs. Au diagrams imply lower nonmetal concentrations in IID that IIIAB. For both groups the slopes on the Pt and W diagrams are lower than those on the Ir–Au diagrams. This trend is found in all magmatic groups, and indicates a higher *D* value for Ir (and Re and Os) than for Pt (and W and Ru). This surely reflects a crystal-chemical difference in the bonding of these trace constituents, but we know of no detailed discussion. The IID-an irons plot at the low-Au end of the IID fields on Figs. 2d–f with the minor exception of W in Arltunga, which would fit better if 10% higher.

Because the two IID irons with anomalous textures plot in or near the trend formed by the other irons on all 10 diagrams shown in Figs. 1 and 2, we are confident that they can be considered to be normal members of the group from

a chemical viewpoint. The process that altered the textures postdated the crystallization of the magma. Their positions at the low-Au extreme of the field implies that they were among the first samples to crystallize. As discussed in some detail in Wasson et al. (2006), in cores in contact with a silicate mantle, crystallization probably proceeded both from the center of the core outwards and from the core-mantle interface inwards. The latter position would probably make them more vulnerable to structural alteration by impacts. However, in the two-liquid model we discuss below, crystallization cannot easily proceed from the outside in because there is no solid surface that the metal can attach to and (and thus avoid buoyant settling).

It is important to note that, any residual metal remaining in the mantle would have the same composition as the first metal to crystallize from the magma. Perhaps this is the preferred origin of these two structurally anomalous irons that have the composition of the earliest solid to form.

Because of the importance of P as a nonmetal that influences solid/liquid distribution coefficients and because of the possibility that the IID magma encountered liquid immiscibility we have plotted P data obtained by Buchwald (1975) by modal integration against Au and also As (because P and As are in the same chemical group) on log–log diagrams (Fig. 3). The increase in P with increasing Au and As is consistent with its incompatibility (and low D_P value). Because some of the observed P was introduced into these meteorites as trapped melt, the observed P concentrations are upper limits on the concentrations of P incorporated in the metallic crystals. We suggest that most of the P values might be high by 20–30%. The plotted data suggest that the trapped melt fraction is lower in the two low-P irons, Arltunga and Losttown.

5. Fractional crystallization of the IID magma: nonmetal concentrations

There are three large, "magmatic" iron-meteorite groups that show large ranges in Ir and negative correlations between Ir and Au, As and Ni on log–log diagrams; IIIAB, accounting for ~31% of known irons, is the largest magmatic group. Fractional crystallization requires complete mixing of the liquid phase on a time scale very short compared to the total crystallization period. In contrast, the nonmagmatic groups such as the IAB main group (Wasson and Kallemeyn, 2002) show relatively small Ir fractionations and, an indication that the liquid chilled quickly, commonly contain chondritic silicates trapped in the metal.

As shown by Scott (1972) the roughly linear arrays that the members of magmatic groups form on log–log diagrams are consistent with formation by fractional crystallization in which the solid/liquid elemental distribution coefficients (the "*D* values") remain roughly constant throughout the crystallization sequence. However, partitioning studies (e.g., Jones and Drake, 1983) in which the common nonmetals S, P and C were included in the system showed that *D* values depend on the concentrations of these elements in the magma. Because most magmatic irons had low concentrations of C and there are relatively few laboratory studies of its effect on *D* values, its effect is generally not modeled (it is, however, of interest that Buchwald (1975) observed graphite in Elbogen and carbides in Carbo). The concentration of Ni also influences the *D* values, but to a lesser extent than the nonmetals. Its effect is also not included in the simulations. Improved analytical data show that the element-Au (or element-Ni) scatter fields, are not linear, but show greater or lesser degrees of curvature.

Neither S nor P is efficiently incorporated into crystallizing metallic iron. As noted in the introduction, we commonly assume that D_S is 0.005. The value of D_P is $\leqslant 0.12$ at S contents <115 mg/g (Chabot and Jones, 2003). Even with a *D* value around 0.12 a very large fraction of the P remains in the melt throughout fractional crystallization.

The nonmetal content of the initial magmas of the magmatic groups has been estimated in two different ways. Jones and Drake (1983), Haack and Scott (1993) and

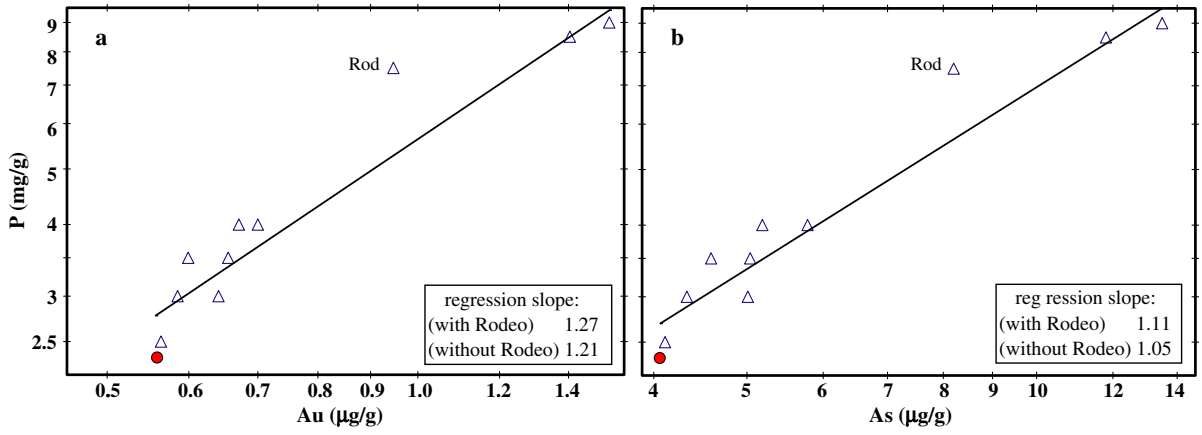

Fig. 3. Log–log plot of P vs. (a) Au and (b) As; P data are from Buchwald (1975). Note that all three elements are incompatible, with P being the least compatible of the three. After allowing for contributions from trapped melt, one can infer that the P content of the initial IID magma was quite high, ca. 14 mg/g. See text for details.

Chabot (2004) plotted the laboratory D values against the S concentrations on log–log diagrams and represented the trends by functions. They then calculated solid crystallization trajectories for different S contents, and selected the S content that yielded the best approximation of the element-Ni or (in Chabot, 2004) element-Au trends through the iron-meteorite groups. The key elements in their tests were Ge, Au and Ir. Chabot and Jones (2003) noted that P and S affected D values similarly and suggested using the same parameters (slopes and intercepts) for both elements. Chabot (2004) estimated the IIIAB initial S content to be 120 mg/g, the same value Haack and Scott (1993) had obtained by a similar method.

Wasson (1999) took a very different approach to estimating the initial S content; he argued that the scatter in experimental D values permit an appreciable range (i.e., within broad bands on plots of log D vs. log nonmetal content) and that a better approach was to maximize the fitting of the observed element-Au trends by trial-and-error adjustment of D values within the limits provided by the laboratory studies. Esbensen et al. (1982) and Wasson (1999) interpreted the wide (factor of 2) range in Ir and Au and the still larger (factor of 9.7) in S observed among the various large (1- to 35-ton) masses of Cape York to indicate melt trapping, and showed that the compositions could be fit if Cape York-Savik contained about ~5% trapped melt and Cape York-Agpalilik contained about ~50% trapped melt. From these data and the modally determined S content of Cape York-Agpalilik of 13.5 mg/g Wasson (1999) estimated an initial S content of 20 mg/g. Our current best estimate is 24 mg/g, 5× lower than that estimated by Chabot (2004).

Unfortunately, the other magmatic groups do not include meteorites with large heterogeneities, i.e., having fragments differing in sulfide contents by similarly large factors. For these groups we make rough estimates of S contents based on mean FeS abundances and the slopes of the inferred solid evolutionary tracks on Ir–Au and Ir–As diagrams. The mean abundance of FeS in the various groups should be roughly proportional to the initial S contents of the magmas.

Neither of these methods of estimating initial S is very precise. Without going into details, it seems that errors of a factor of 2 or larger are possible.

In this paper we follow the general approach of Wasson (1999) and search for algorithms relating D values to nonmetal concentrations that lead to plausible explanations of the observed-trends. As in most of our recent papers, we limit our detailed modeling efforts to the Ir–Au and Ir–As scatter diagrams. We use the simplified approach of Chabot and Jones (2003), and we used their equations to relate D values to Fe "domains" (i.e., the fraction of Fe not bound to S or P calculated by their equation 7). We calculated our D values using their wt% formalism.

The trends within the group provide several clues regarding the crystallization process. On Ir–Au and Ir–As diagrams the left envelope of the scatter field provides the best estimate of the solid track of the crystallizing magma. The right envelope provides a lower limit of the liquid track. The positions of each meteorite along equilibrium mixing curves connecting to solid and liquid tracks provide estimates of the fraction of trapped liquid, and it is obvious that a satisfactory choice of D_{Au} and D_{As} algorithms should yield similar estimates for the fraction of trapped melt for each meteorite on Ir–Au and Ir–As diagrams.

Buchwald (1975) observed very low FeS abundances in IID sections and especially in Wallapai, the most evolved member of the group. For this reason, we assume that Wallapai and the closely related Needles iron have low contents of trapped melt, i.e., that they plot near the solid evolutionary track. This required that D_{Ir}, D_{Au} and D_{As} values be relatively low and thus that nonmetal concentrations are relatively low, consistent with the general IID observations by Buchwald summarized earlier. Buchwald's modally estimated P concentrations are high, but not high enough to produce steep slopes on Ir–Au or Ir–As diagrams). In our IID modeling we assumed an initial IID S content 7 mg/g, close to the value of 6 mg/g used by Wasson et al. (2006) for group IVA. And, as discussed below, we used a P content of 14 mg/g, higher than the values previous inferred for IVA and IIIAB.

In Table 3 we list the parameters used in calculating solid and liquid tracks fitted to the IID Ir–Au and Ir–As scatter fields (Fig. 4). Also listed are the similar values of these parameters proposed by Chabot and Jones (2003).

Not surprising for such a small group, there are large gaps in the IID compositional space. Examination of Fig. 4 shows that the positions of 16 of 19 IID irons correspond to degrees of crystallization of 40% or less. The most evolved iron, Wallapai, plots at a degree of crystallization of 73%. It appears that most of the IID cumulate was broken up to liberate meteoroids, but that stochastic effects caused the vast majority of the collected meteorites to be products of the first 40% of crystallization.

A measure of the success of our modeling approach is whether irons occupy the same relative position on each diagram. It is important to know that sampling of the metallic phases cannot affect this test because Au concentrates in taenite and As in kamacite. We illustrate this test with two examples. In Figs. 4a and b the IID iron plotting just above the 50% mixing curves is Rodeo; on the Ir–Au diagram its position implies ~5% trapped melt, on the Ir–As plot the implied melt fraction is ~7%. The IID iron showing the highest apparent melt fraction is Mount Ouray; on both the Ir–Au and Ir–As plots the inferred melt fraction is 12–13%. From these two examples we conclude that both irons have a minor trapped melt component and that our D_{Au} and D_{As} values are in good relative agreement. Note, however, that we could have chosen other D_{Au} and D_{As} values that would have yielded melt fractions differing by as much as 2–3%.

Table 2
Initial compositions of the IID, IVA and IIIAB magmas inferred from distributions on log element-log Au diagrams; IVA and IIIAB values taken from Wasson and Richardson (2001)

Element	IID	IVA	IIIAB	CI	IID/CI	IVA/CI	IIIAB/CI
P (mg/g)	17.8	1.30	3.75	1.02	1.30	0.163	0.471
Cr (μg/g)	230	830	352	2650	0.009	0.040	0.017
Co (mg/g)	6.98	3.99	5.09	0.550	1.29	0.93	1.19
Ni (mg/g)	105	83.4	83.6	10.7	≡1.000	≡1.000	≡1.000
Cu (μg/g)	255	280	143	121	0.215	0.297	0.151
Ga (μg/g)	82.8	2.97	18.5	9.8	0.86	0.039	0.242
Ge (μg/g)	100.5	0.160	36.4	33	0.310	0.0006	0.141
As (μg/g)	15.0	13.4	9.69	1.84	0.831	0.933	0.674
Sb (ng/g)	137	3.3	50.2	153	0.091	0.003	0.042
W (μg/g)	2.63	0.55	0.952	100	2.68	0.706	1.218
Re (ng/g)	1100	200	364	41	3.03	0.693	1.260
Ir (μg/g)	10.5	1.88	4.10	0.46	2.33	0.525	1.140
Pt (μg/g)	17.4	4.7	8.01	0.99	1.79	0.610	1.036
Au (μg/g)	1.60	2.25	1.17	0.180	0.91	1.60	0.83

CI data from Wasson and Kallemeyn (1988) but with Co, Re and Au increased 10–20% to make the overall iron-meteorite trends smoother. The three right columns give abundances normalized to Ni and CI.

6. Elemental abundances in group IID; abundant volatiles save one

In Fig. 4 we illustrated how solid/liquid distribution coefficients can be inferred from element/Au (or element/As) diagrams by assuming that the left envelope of the data corresponds to irons containing negligible amounts of trapped melt and fitting a solid evolutionary track to it. As discussed in the Section 5, this exercise requires making various assumptions. The final result is that one obtains solid and liquid tracks, and the initial composition of the core is then given by the high-Ir end of the calculated liquid tracks.

As first discussed by Scott (1972) this approach offers a good way to estimate the initial compositions of the cores that produced the iron meteorite groups provided that our terrestrial sample of the group includes samples of the first materials to crystallize. Several of the IID irons have exceptionally high Ir contents, evidence that some of the earliest crystallized irons are included in our sample set; this is the more important because the modeling of the

Table 3
Values of parameters used to calculate the IID solid and liquid tracks shown in Fig. 4

Element	D_0 this work	D_0 Chabot/Jones	β this work	β Chabot/Jones
As	0.196	0.22	2.00	2.2
Ir	1.81	1.5	4.6	4.9
Au	0.265	0.25	2.26	2.0

Parameters recommended by Chabot and Jones (2003) shown for comparison.

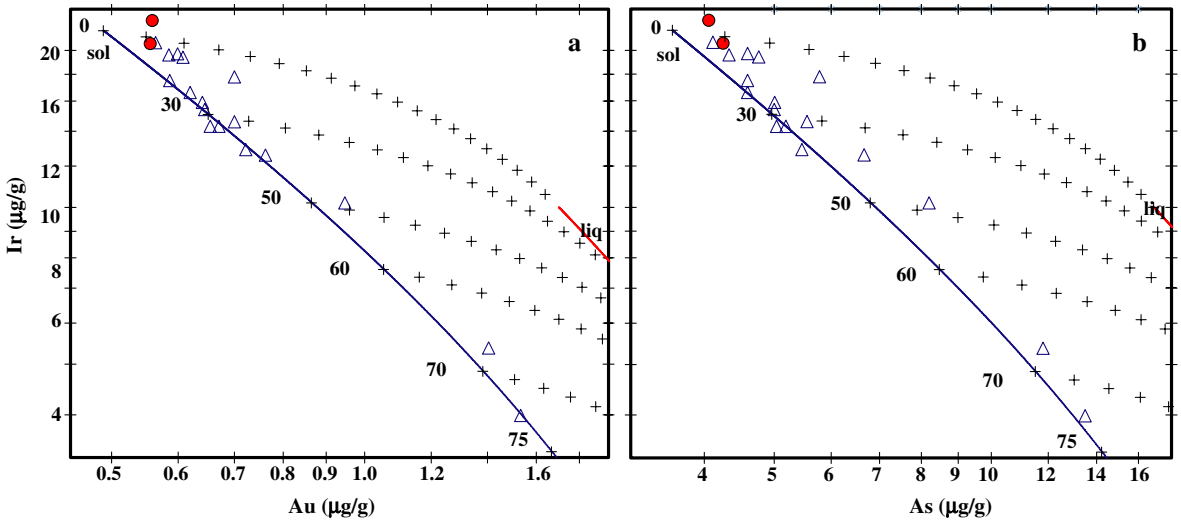

Fig. 4. Log–log plots of Ir vs. (a) Au and (b) As for IID irons. Estimated solid and liquid tracks are shown; most IID data plot near the solid track. Solid–liquid mixing curves are shown at 0, 30, 50, 60, 70 and 75% crystallization; the distances between adjacent crosses corresponds to 5% differences. The relatively low D_{Ir}, D_{Au} and D_{As} values used to fit the trends imply that the S content of the initial magma was quite low, similar to that in group IVA.

Ir–Au and Ir–As trends imply relatively low D_{Ir} values, and thus high Ir in the initial magma.

We followed the simple approach used by Wasson and Richardson (2001) to estimate the initial elemental concentrations of the IVA and IIIAB magmas. They roughly fit a line segment to the irons at the low-Au extreme of the group (avoiding irons showing evidence of significant degrees of melt trapping) and extrapolated it to the Au content of the first solid obtained by fractional crystallization modeling. This gives $E_{sol,i}$, the concentration of the element in the first solid to crystallize. If the D values are essentially constant (as they are expected to be during the first 20% of magma crystallization) the slope of the line segment is $(D_{El} - 1)/(D_{Au} - 1)$ thus the value of D_{El} can be obtained from the slope and the value of D_{Au} previously obtained by modeling. The elemental concentration in the initial magma, $E_{liq,i}$, is given by the relationship:

$$E_{liq,i} = E_{sol,i}/D_{El}$$

In Table 2 the estimated elemental concentrations in group IID are compared with those in two other magmatic groups, IVA and IIIAB. Also listed are Ni and CI-chondrite normalized abundance ratios; these are plotted in Fig. 5 roughly in order of decreasing condensation temperature (Wasson, 1985; Lodders and Fegley, 1998), i.e., increasing volatility. The IVA and IIIAB estimates are taken from Wasson and Richardson (2001); we increased their IIIAB Cu abundance by 60%, however, reflecting newer views about dealing with the scatter and the uncertain chemical behavior of this element. The striking observation in Table 2 and Fig. 5 is the fact that, compared to groups IVA and IIIAB, the IID initial melt has the highest abundances of all refractory and four out of seven volatile siderophiles. Chromium is the only element having an appreciably lower abundance ratio in IID compared to the other groups; the abundance ratio would have been lower had we assumed a D_{Cr} higher than 0.5.

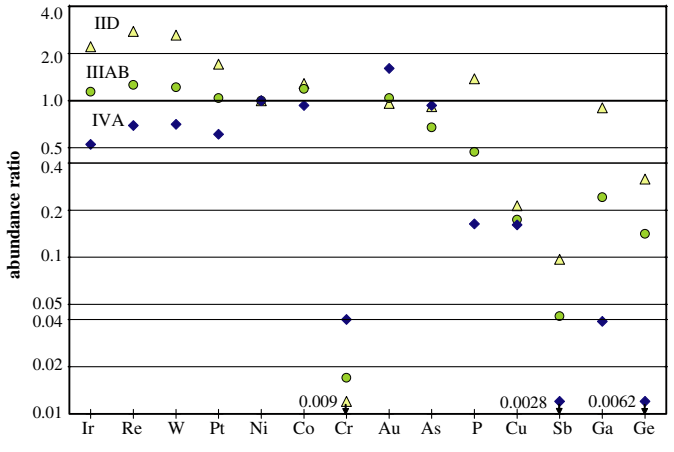

Fig. 5. Ni and CI-chondrite normalized abundances in groups IID, IIIAB and IVA for elements included in this study. Elements are plotted in approximate order of volatility increasing to the right. Group IID has the highest abundance of refractory elements and the highest abundance for four of the seven volatiles (Au through Ge).

As listed in Table 2, we estimated the P content of the IID initial magma to be 14 mg/g. To make this estimate we had to make a correction for the fraction of the observed P that entered the IID irons as trapped melt. We assumed that this effect elevated the lowest P values (in Arltunga and Losttown) by ~5%, but elevated those in other low-Au IID irons by 20–30%.

The Fe–P phase diagram (Brandes and Brook, 1998) shows a liquidus temperature of ~1500 °C (1773 K) for 14 mg/g P. The actual liquidus temperature would be lowered about 20–26 K by the presence of 105 mg/g Ni and ~10 K by the presence of 7 mg/g S. Thus our best estimate of the initial IID liquidus temperature is 1740 K. For comparison, the Fe–FeS eutectic temperature is ca. 1260 K and that estimated for the low-P, low-S IVA magma is 1760 K (Wasson et al., 2006).

7. Depletion of S in IID by independent separation of metallic liquids

We have recognized only two processes that can explain low S contents in a meteoritic metallic magma—volatile loss and loss of a S-rich melt. Because, as shown in Fig. 5, all volatiles except S were relatively abundant in the IID magma, it seems unlikely that the depletion of S was the result of volatility. We therefore focused on the loss of a S-rich liquid. The two possibilities are liquid immiscibility (Ulff-Møller, 1998a,b) or the closely related process discussed by Kracher and Wasson (1982), two extractions from the same chondritic mantle source, with essentially all the FeS entering the first extraction. Because the second metallic liquid is much denser than the first, FeS-rich liquid, Kracher and Wasson (1982) infer that bodies of metal would create channels through the latter and form an inner core. They also noted that, even if the two liquids are miscible, mixing across the interface would have been a slow process, and the two-layer structure would have been metastable for ~1 Ma.

The role of liquid immiscibility in the crystallization of iron-meteorite magmas was discussed in some detail by Ulff-Møller (1998b). Chabot and Drake (2000) reported several phase equilibrium runs for systems involving liquid immiscibility. Both give an inferred boundary separating the Fe-solid + 1-liquid field from the Fe-solid + 2-liquid field. At high temperatures there is complete miscibility in the Fe–S–P system. According to Schürmann and Neubert (1980) the critical point is located at 1553 K above which no solid can coexist with two immiscible liquids. At this point the two liquids have nearly identical compositions (152 mg/g S, 6 mg/g P). At higher temperatures there can still be immiscibility but the size of the miscibility gap shrinks with increasing temperature and finally disappears around 2000 K.

We discussed above that the first (low-Au, high-Ir) IID irons crystallized from a magma with a high (14 mg/g) P content, high volatile (e.g., Ga) contents but a low (~7 mg/g) S content, and that the liquidus temperature of this magma was ~1740 K. Because, at this temperature and composition, immiscibility cannot be invoked to explain the separation of a S-rich liquid, we conclude that the Kracher and Wasson (1982) model in which two liquids form metastably is the preferred scenario for explaining the depletion of S in this volatile-rich group.

In our recent paper on the IVA irons (Wasson et al., 2006) we argued that rapid impact heating was the most plausible mechanism for explaining the large fractional loss of S and the most volatile siderophiles from this group. In contrast, slow internal heating (e.g., by the decay of ^{26}Al and/or ^{60}Fe) offers a more plausible way to produce two episodes of metallic melt extraction with minimal loss of volatiles.

Kita et al. (2000) and Kunihiro et al. (2004) reported that studies of ordinary-chondrite and carbonaceous-chondrite chondrules showed relatively low initial ^{26}Al/^{27}Al ratios. Kunihiro et al. (2004) showed that the amounts of ^{26}Al are too low to melt and differentiate asteroids formed from these materials and suggested that heating by short-lived radionuclides might not be generally responsible for the melting that produced differentiated meteorites. However, they and others (e.g., Kleine et al., 2005) have noted that, if asteroids formed ~1 Ma earlier, these could have been melted by ^{26}Al. The decay of ^{60}Fe may also have played an important role. The ^{60}Fe/^{56}Fe present in LL3.1 Bishunpur and Krymka was reported to be 1.4×10^{-7} by Tachibana and Huss (2003) but much higher, 9.2×10^{-7}, by Mostefaoui et al. (2005). If the higher ^{60}Fe/^{56}Fe ratio is correct and if asteroids formed soon after the formation of chondrules (^{26}Al) and troilite (^{60}Fe), then our calculations show that the combination of the two radioisotopes could melt and differentiate asteroids.

We suggest the following scenario. As temperatures gradually rose in a metal-rich and volatile-rich chondritic asteroid the FeS and a minor fraction of the metal melted to form the FeS–Fe eutectic at ~1260 K. The temperature continued to increase until the melt fraction again became large enough to separate and drain down to the center of the asteroid. Because the asteroid was probably highly porous (reflecting a combination of nebular accretionary porosity and "rubble-pile" impact-induced fracturing), the minimum fraction of melt that could drain down to form a S-rich core may have been small. The S content of the melt may have been only slightly lower that the eutectic value of ~315 mg/g. If the chondritic precursor had an S content of ~30 mg/g, similar to that in CM chondrites, the fraction of the chondritic parental materials present as melt may have been ~100 mg/g at the time of separation. This might have occurred at a temperature of 1260–1300 K.

At this point no silicate melt had formed. When the temperature reached ~1450 K a basaltic melt separated and removed most of the remaining ^{26}Al from the mantle. At this temperature the materials were relatively plastic and the remaining porosity presumably disappeared. Heating of the mantle continued, but the heat source was now mainly ^{60}Fe which has a half-life of 1.5 Ma, about twice that of ^{26}Al. Heating continued until the temperature reached ~1740 K (or higher) at which point the remaining metallic melt collected into pools that became gravitationally unstable and separated to form an inner core, passing through the S-rich melt that had initially separated. Kracher and Wasson (1982) suggest that these dense melts rapidly transited the S-rich liquid, assimilating only a minor fraction on the way down.

The first metal extracted from the chondritic parental materials contained nearly all the S and enough Fe metal to reach the eutectic composition. It had low element/Fe ratios for most elements, possible exceptions being Cu and Cr. The second, P-rich metal would thus have had enhanced element/Fe ratios for the elements having high D values at the time the early S-rich melt formed and separated. The uniformly high abundances of refractory siderophiles in group IID are consistent with this picture.

8. Coexistence and evolution of dual cores in the IID asteroid

Kracher and Wasson (1982) noted that crystallization of the inner core would produce a stagnant boundary layer near the interface between the two magmas, and that transport of matter and heat across the interface would be entirely by diffusion, even if the two cores were internally convecting. They estimated that the mass diffusivity of Fe or Ni in molten metal at 1700 K is $\sim 10^{4.5}$ cm^2 s^{-1}. This leads to a mean diffusion length $(D \cdot t)^{1/2}$ of 300 m in 1 Ma. Most other elements (including S) would have had similar or lower mass diffusivities.

We know that the IID magma was convecting, otherwise the group would not show clear evidence of fractional crystallization. It is possible that the outer core did not convect. Because the thermal conductivity of the high-S melt was roughly 30× higher than that of the overlying silicate mantle, dimensional arguments suggest that the temperature drop across a conducting outer core was ~10 K. In a pure liquid this could produce convection but, because diffusion was gradually adding Fe to the base of the outer core, the density gradient soon became great enough to prevent convection within a basal layer that gradually increased in thickness.

According to this picture, the IID irons formed by crystallization of the inner P-rich "metallic" liquid. As discussed above, the first solid would have precipitated from this liquid at ~1740 K. As a result of the crystallization of the metallic (inner core) liquid, its P and S content increased and the temperature fell. After about 60% crystallization of the inner core the P content had reached ~40 mg/g and the S content ~20 mg/g and the temperature had fallen low enough that the two liquids became truly immiscible. However even after achieving immiscibility,

the two liquids did not equilibrate because of limited exchange at the interface.

Because there was no structure to support dense crystallizing metal at the upper surface, the inner core could only crystallize from the center outwards. It mixed by convection, as necessary to keep the liquid well stirred during fractional crystallization. The main heat source driving the convection was probably the latent heat of crystallization. As discussed above the lowest layer of the outer core did not convect. Whether the main body convected depends on the rate of heat transport and the nature of compositional gradients that are not easily modeled.

To help the reader picture our model we offer the following scenario. A highly porous asteroid (thus having low thermal conductivity) with a radius R of 20–50 km became hot enough to raise a region with radius $r = 0.5R$ to a temperature of ~1300 K. The resulting eutectic melt drained through the porous solids to the center of the asteroid and formed an S-rich core.

Temperatures continued to rise and, at a temperature of ~1450 K a basaltic melt formed and ascended buoyantly. It interacted with adjacent solids and cooled by assimilation and conduction; it may have stopped migrating near the top of the zone from which the S-rich melt was extracted. If there was still a thick layer of insulating material above it, heat produced by ^{26}Al decay could have still contributed to the thermal budget of the materials below it. Most of the asteroid (that between the surface and $r = 0.5R$) did not melt.

Temperatures in the interior continued to rise, and became high enough in the lower portion of the melt-depleted zone to melt the remaining metal. This melt collected into pools that became unstable and drained to form the inner core.

For convenience we assume that the amount of combined metallic melts that could be extracted from the original chondritic matter was 220 mg/g, and that each extraction removed 110 mg/g. However, the original mass of chondritic material that produced the late, P-rich melt was much smaller (perhaps 5×) than the mass that had produced the S-rich melt. After allowance for the difference in density (~7.4 g cm^{-3} for the P-rich magma, ~4.3 g cm^{-3} for the S-rich magma (Kaiura and Toguri, 1979)), we obtain a volume of the outer core that was ~7× larger than that of the inner core. An asteroid with a radius of 20 km and an initial porosity of 50% could have produced an inner core with a radius of ~3 km and a combined core with a radius ~6 km.

As noted above, diffusion could only transport Fe, Ni and similar elements ~300 m in 1 Ma. Because diffusion gradually increases the thickness of the stagnant layers at the bottom of the outer core and at the top of the inner core, our model implies that there would have been little contamination of the convecting lower portion of the inner core during a lifetime as long as 1 Ma. Any chromite (density 4.8–5.0 g cm^{-3}) that formed in the body of the liquid would have risen buoyantly to the stagnant zone between the two cores, but was denser than the upper core. We picture that this formed a slurry, but that the grains coarsened with time. Small amount of metal were entrained upwards with the chromite The chromite layer would also have served as a diffusional barrier between the magmas. In a relatively small asteroid diffusional exchange may have been slow enough to allow the inner core to crystallize to the degree (~75%) required to account for the observed set of IID irons.

9. Two metal extractions; implications regarding element partitioning

If the above scenario involving the extraction of two melts from the IID mantle is correct, the inferred initial composition of the IID mantle has implications regarding the distribution of elements between the S-rich melt and the residual, refractory metal solids. We have suggested that the heat source was internal and slow, requiring $\geqslant$1 Ma (following formation of the asteroid) for the temperature of to rise high enough (to ca. 1300 K) to produce a volume of metal that could gravitationally separate to form the first core. Under such slow heating conditions it is clear that there would have been equilibrium between the melt and the residual millimeter-size metal grains in the chondritic parental material.

Chabot and Jones (2003) reviewed element partitioning data for the systems involving Fe, Ni and nonmetals. In most of the experiments the nonmetal is S, with a minor fraction involving P and relatively few involving C. In this data set they report that increasing the S contents causes the D values of all studied elements to increase except Cr, Cu and Ag. D_{As} and D_{Au} increase from values smaller than 0.3 at low S contents to values >1 at S mole fractions > 0.3 (although there is much scatter in the Au data). As a result, one would predict that, at the time the S-rich magma separated, the concentration ratio (residual metal/S-rich melt) should have been near unity or above for all elements in our study except Cu and Cr.

Assuming that the bulk of these elements remained in the residual metal and that the mass of the S-rich melt was similar to or smaller than the mass of the residual metal, the prediction is that, in the residual metal, element/Fe or element/Ni ratios for all elements except Cu and Cr should be the same or higher that those in the chondritic precursor material. The abundance data plotted in Fig. 5 are consistent with this interpretation. Only Cr, Cu and Sb show appreciable depletions relative to CI-chondrite abundances. A few laboratory partitioning studies of Sb reported by Chabot et al. (2003) indicate that it also largely partitioned into the S-rich melt.

An interesting question is whether there are iron meteorites in our collections that could be samples of the proposed S-rich outer core of the IID parent. An obvious prediction would be that these should, on average, have high S contents. Some melt was always trapped during the crystallization of metal, and the higher the S content

of the melt, the higher the expected mean FeS content compared to other iron-meteorite groups. In addition, the viscosity of S-rich melts is expected to be appreciably higher than those of low-S melts (Dobson et al., 2000), thus hindering the ability of cumulates to free themselves of melt. Similar arguments would suggest high Cu and Cr in the FeS inclusions present in irons crystallizing from the S-rich magma.

Although one might intuitively expect the Ir content of the initial metal crystallized from the high-S melt to be low, a consequence of our model is that the first metal to crystallize from this melt would have the same composition as the initial melt parental to the IID irons, i.e., ~10.5 μg/g Ir.

At this time we have no irons to propose as possible samples of the S-rich magma. The reason may be that these have shorter space-erosion lifetimes compared to irons with low-FeS contents (Kracher and Wasson, 1982). And those that formed at or near the Fe-FeS eutectic may have formed quite small (perhaps centimeter-size) metallic regions that fall on Earth as tiny nuggets and rarely become named meteorites.

10. Summary

Studies of 19 of the 21 members of the magmatic iron meteorite group IID show trends consistent with the fractional crystallization of a low-S metallic magma. The two IID irons with the lowest Au and highest Ir contents have anomalous metallic structures but their concentrations are normal with minor exceptions.

Buchwald (1975) had called attention to the low-S contents observed in sections of IID irons. We observe low negative slopes on plots of log Ir vs. log-Au or log-As, an indication that the S content of the initial magma was low. We suggest that it was similar to that in the initial magma of group IVA; our best estimate is 7 mg/g S in the initial magma, but this estimate has a relatively high uncertainty. We estimate a P content of 14 mg/g. Most of the IID data plot near our best estimate of the solid crystallization track implying that amounts of trapped melt were low (<14%). The initial solid/liquid distribution coefficient for Ir inferred from the slope is ~2, as expected for a magma having a low nonmetal content.

Group IID has high contents of most volatile elements. Its Ga content is the highest known in a magmatic iron meteorite suggesting a high volatile content in the chondritic precursor material. There are two ways to lose S, by volatilization (the probable mechanism in group IVA) and by extraction of a low-temperature S-rich melt. Since volatiles other than S are abundant in group IID, we infer that the S was lost by extraction into an early formed, S-rich melt. The parental magma of the IID irons would then represent a second extraction that penetrated through the S-rich melt and formed an inner core, a mechanism first proposed by Kracher and Wasson (1982). The initial liquidus temperature of this low-S, high-P magma is estimated to have been 1740 K.

To achieve two extractions from the same mantle requires slow heating, as would result if the heat source consisted of the short-lived radionuclides ^{26}Al and/or ^{60}Fe. Wasson et al. (2006) noted that simple modeling arguments indicate that impact heating is effective at producing volatile loss whereas internal heating is not, consistent with an internal source being responsible for heating and melting the group-IID asteroid.

Kracher and Wasson (1982) observed that each core would have had a stagnant boundary layer near the mutual interface, and thus that elemental and heat transport between them would have been by diffusion. Diffusion of S downwards and Fe upwards would have increased the thickness of this boundary layer. A chromite layer formed within the stagnant zone would have further hindered exchange.

Although the crystallization of the outer, S-rich core would also have produced Fe–Ni metal, much of this material crystallized at the metal-FeS eutectic, and the resulting metal domains may have been so small that they did not survive to fall as meteorites or, if they fell, were too small to be classified as a named meteorite.

Acknowledgments

We thank Finn Ulff-Møller, Byeon-Gak Choi, Eric Jerde, Xinwei Ouyang, John Richardson, Greg Kallemeyn, Dan Malvin, John Willis and Jianmin Wang for assistance in gathering the INAA data. A number of curators provided samples. We are indebted to Nancy Chabot, Mary Horan, Finn Ulff-Møller and Andrew Campbell for constructive reviews. Technical support was provided by Eileen Block, Bo Kim and Phuong Dang. This research was mainly supported by NASA Grant NAG5-12058.

Associate editor: Alan D. Brandon

Appendix A. Supplementary data

Supplementary data associated with this article can be found, in the online version, at doi:10.1016/j.gca.2006.01.032.

Appendix B. Replicate data

In Table A1 we list individual analyses of IID irons. As discussed in the experimental section, early INAA runs that did not include a Filomena standard (those completed before 1981) have been reevaluated including, in most cases, the use of two or more of the analyzed meteorites as "proxy standards" based on more recent replicates. The second column gives the year and month of analysis.

The data obtained after 1986 are more accurate and precise that the earlier data. When replicates differed in vin-

Table A1
Alphabetical list of replicate INAA data for IID irons

Meteorite	Date	Cr (μg/g)	Co (mg/g)	Ni (mg/g)	Cu (μg/g)	Ga (μg/g)	As (μg/g)	Ru (μg/g)	W (μg/g)	Re (ng/g)	Ir (μg/g)	Pt (μg/g)	Au (μg/g)
Alt Bela	7611	116	6.40	115.0	276	70.9	4.25		2.93	1570	16.6		0.612
Alt Bela	7709	48	6.69	97.1	299	74.9	4.65		2.65	1866	16.6		0.623
Arltunga	0404	118	6.44	94.6	249	65.9	3.92	18.3	2.76	1994	20.5	20.2	0.554
Arltunga	0407	124	6.35	98.9	278	72.3	4.19	21.2	2.96	2145	20.7	22.9	0.563
Bridgewater	0307	308	6.67	98.4	286	77.9	4.81		3.11	2010	19.9	20.7	0.599
Bridgewater	0309	96	6.61	101	261	70.7	4.36		2.85	2023	19.5	22.9	0.599
Brownfield (1966)	0302	53	6.74	99.3	288	77.6	5.59		3.15	1317	12.7	20.8	0.710
Brownfield (1966)	0304	39	6.72	98.1	270	73.1	5.06		2.75	1202	13.0	19.3	0.734
Carbo	0212	23	6.72	103.3	355	75.7	5.26		3.77	1420	14.4	20.2	0.679
Carbo	0302	153	6.66	100.0	303	77.8	5.11		3.10	1422	14.2	24.6	0.662
Cheder	0411	—	6.59	102.9	255	71.2	4.45	19.9	2.84	1554	17.4	18.2	0.586
Cheder	0412	54	6.64	97.7	279	71.8	4.73	20.0	3.15	1682	17.5	22.2	0.586
Elbogen	8809	34	6.69	102.5	262	74.1	5.10		2.83	1429	15.5	16.7	0.638
Elbogen	0212	63	6.70	97.6	274	74.0	4.96		2.96	1660	16.1	20.1	0.643
Hraschina	8809	32	7.03	107.4	312	80.6	5.57		2.26	1179	12.7	17.3	0.721
Hraschina	0212	122	6.74	96.4	286	75.5	5.53		2.85	1764	16.5	21.9	0.679
Losttown	7701	<100	6.62	99.8		70.8	4.21		3.10	1986	20.4		0.569
Losttown	7709	67	6.56	102.0	314	75.8	3.92		3.29	2356	20.4		0.551
Losttown	0011	35	6.60	98.2	273	70.1	4.15		2.98	1976	20.8	19.3	0.568
Mafuta	0008	62	6.72	99.7	269	73.4	4.92		2.97	1465	15.5	22.1	0.656
Mafuta	0009	62	6.71	100.9	259	71.9	5.08		2.86	1314	15.3	17.4	0.634
Mount Ouray	0302	93	6.73	99.8	258	73.0	5.63		3.37	1726	17.5	23.3	0.687
Mount Ouray	0304	79	6.65	97.8	272	74.8	5.93		2.99	1761	18.1	22.7	0.713
Needles	9001	32	7.07	103.8	252	86.7	11.8		2.13	465	5.33	14.7	1.401
Needles	9003	30	6.94	108.4	245	84.5	11.7		2.24	550	5.41	11.8	1.407
N'Kandhla	0302	76	6.69	94.0	249	70.3	4.19		3.22	1928	19.3	21.3	0.574
N'Kandhla	0304	60	6.82	97.9	257	72.2	4.47		2.84	1956	19.9	18.4	0.595
NEA002	0504	148	6.56	101.7	258	70.7	4.09	19.8	3.06	2380	22.8	22.4	0.551
NEA002	0508	116	6.60	102.7	259	70.4	4.40	20.7	2.96	2320	22.4	22.3	0.561
Puquios	0302	77	6.76	95.0	247	75.3	4.98		2.97	1405	14.4	20.1	0.651
Puquios	0304	18	6.58	103.5	279	77.4	5.10		5.11	1381	14.2	19.7	0.659
Rodeo	0212	137	6.91	105.4	269	75.3	8.15		2.42	1196	10.6	15.7	0.973
Rodeo	0302	139	6.84	104.1	237	74.9	8.24		2.49	935	9.78	15.3	0.921
St. Augustine	0004	58	6.69	98.4	285	75.4	4.66		3.01	1950	19.4	25.7	0.608
St. Augustine	0006	112	6.63	102.6	246	73.9	4.86		3.20	2001	19.3	18.9	0.608
Vicenice	8510	111	6.75	101.1	284	79.7	7.00		2.86	1129	12.9		0.763
Vicenice	8511	59	6.81	100.1	296	75.0	6.62		3.04	1317	12.8		0.768
Vicenice	8809	38	6.70	101.7	256	75.3	6.54		2.83	1057	12.2	16.7	0.754
Wallapai	9001	31	6.83	113.6	245	86.3	13.8		2.14	334	3.77	12.9	1.512
Wallapai	9003	33	6.98	107.7	236	83.6	13.2		1.99	490	4.36	10.2	1.554

This table available in digital form in electronic annex EA.

tage we assigned double weight to those from 1986 or later in determining the means.

Although we assign values to Ge and Sb as part of our INAA studies, most values for group IID are upper limits and the ones for which we recorded nominal values have high (10–20%) uncertainties. We therefore did not include them in Table A1.

References

Brandes, E.A., Brook, G.B., 1998. *Smithells Metal Reference Book*. Butterworth-Heinemann, CA, p. 1600.

Buchwald, V.F., 1975. *Handbook of Iron Meteorites*. University of California Press, Los Angeles, pp. 1418.

Chabot, N.L., 2004. Sulfur contents of the parental metallic cores of magmatic iron meteorites. *Geochim. Cosmochim. Acta* **68**, 3607–3618.

Chabot, N.L., Drake, M.J., 2000. Crystallization of magmatic iron meteorites: the effects of phosphorus and liquid immiscibility. *Meteorit. Planet. Sci.* **35**, 807–816.

Chabot, N.L., Jones, J.H., 2003. The parameterization of solid metal-liquid metal partitioning of siderophile elements. *Meteorit. Planet. Sci.* **38**, 1425–1436.

Chabot, N.L., Campbell, A.J., Jones, J.H., Humayun, M., Agee, C.B., 2003. An experimental test of Henry's law in solid metal-liquid metal systems with implications for iron meteorites. *Meteorit. Planet. Sci.* **38**, 181–196.

Dobson, D.P., Chricton, W.A., Vocaldo, L., Jones, A.P., Wang, Y., Uchida, T., Rivers, M., Sutton, S., Brodholt, J.P., 2000. In situ measurement of viscosity in liquids in the Fe-FeS system at high pressures and temperatures. *Am. Mineral.* **85**, 215–225.

D'Orazio, M., Folco, L., 2003. Chemical analysis of iron meteorites by inductively coupled plasma-mass spectrometry. *Geostan. Newslett.* **27**, 215–225.

Esbensen, K.H., Buchwald, V.F., Malvin, D.J., Wasson, J.T., 1982. Systematic compositional variations in the Cape York iron meteorite. *Geochim. Cosmochim. Acta* **46**, 1913–1920.

Haack, H., Scott, E.R.D., 1993. Chemical fractionations in group IIIAB iron meteorites: origin by dendritic crystallization of an asteroidal core. *Geochim. Cosmochim. Acta* **57**, 3457–3472.

Jones, J.H., Drake, M.J., 1983. Experimental investigations of trace element fractionations in iron meteorites, II: the influence of sulfur. *Geochim. Cosmochim. Acta* **47**, 1199–1209.

Jones, J.H., Malvin, D.J., 1990. A nonmetal interaction model for the segregation of trace metals during solidification of Fe-Ni-S, Fe-Ni-P, and Fe-Ni-S-P alloys. *Metall. Trans.* **21b**, 697–706.

Kaiura, G.H., Toguri, J.M., 1979. Densities of the motel FeS, FeS-Cu_2S and Fe-S-O systems- utilizing a bottom-balance archimedean technique. *Can. Metall. Quart.* **18**, 155–164.

Kita, N.T., Nagahara, H., Togashi, S., Morishita, Y., 2000. A short duration of chondrule formation in the solar nebula: evidence from ^{26}Al in Semarkona ferromagnesian chondrules. *Geochim. Cosmochim. Acta* **64**, 3913–3922.

Kleine, T., Mezger, K., Palme, H., Scherer, E., Munker, C., 2005. Early core formation in asteroids and late accretion of chondrite parent bodies: Evidence from ^{182}Hf–^{182}W in CAIs, metal-rich chondrites and iron meteorites. *Geochim. Cosmochim. Acta* **69**, 5805–5818.

Kracher, A., Wasson, J.T., 1982. The role of S in the evolution of the parental cores of the iron meteorites. *Geochim. Cosmochim. Acta* **46**, 2419–2426.

Kunihiro, T., Rubin, A.E., McKeegan, K., Wasson, J.T., 2004. Initial ^{26}Al/^{27}Al in carbonaceous-chondrite chondrules: too little ^{26}Al to melt asteroids. *Geochim. Cosmochim. Acta* **68**, 2947–2957.

Lodders, K., Fegley, B.J., 1998. *The Planetary Scientist's Companion*. Oxford University Press, New York, p. 371.

Marvin, U.B., 1962. Cristobalite in the Carbo iron meteorite. *Nature* **196**, 634–636.

Mostefaoui, S., Lugmair, G.W., Hoppe, P., 2005. ^{60}Fe: a heat source for planetary differentiation from a nearby supernova explosion. *Astrophys. J.* **625**, 271–277.

Scott, E.D., Wasson, J.T., 1975. Classification and properties of iron meteorites. *Rev. Geophys. Space Phys.* **13**, 527–546.

Scott, E.R.D., 1972. Chemical fractionation in iron meteorites and its interpretation. *Geochim. Cosmochim. Acta* **36**, 1205–1236.

Schürmann, E., Neubert, V., 1980. Schmelzgleichgewichte in den eisenreichen Ecken der Dreistoffsysteme Eisen-Schwefel-Kohlenstoff, Eisen-Schwefel-Phosphor und Eisen-Schwefel-Silicium. *Giessereiforschung* **32**, 1–5.

Tachibana, S., Huss, G.R., 2003. The initial abundance of ^{60}Fe in the solar system. *Astrophys. J.* **588**, L41–L44.

Ulff-Møller, F., 1998a. Solubility of chromium and oxygen in metallic liquids and the co-crystallization of chromite and metal in iron meteorite parent bodies (abstract). *Lunar Planet. Sci.* **29** (abstract 1568).

Ulff-Møller, F., 1998b. Effects of liquid immiscibility on trace element fractionation in magmatic iron meteorites: a case study of group IIIAB. *Meteorit. Planet. Sci.* **33**, 207–220.

Wasson, J.T., 1969. The chemical classification of iron meteorites–III. Hexahedrites and other irons with germanium concentrations between 80 abd 200 ppm. *Geochim. Cosmochim. Acta* **33**, 859–876.

Wasson, J.T., 1985. *Meteorites: Their Record of Early Solar System History*. Freeman, pp. 267.

Wasson, J.T., 1999. Trapped melt in IIIAB irons; solid/liquid elemental partitioning during the fractionation of the IIIAB magma. *Geochim. Cosmochim. Acta* **63**, 2875–2889.

Wasson, J.T., Kallemeyn, G.W., 1988. Compositions of chondrites. *Phil. Trans. R. Soc. Lond. A* **325**, 535–544.

Wasson, J.T., Kallemeyn, G.W., 2002. The IAB iron-meteorite complex: a group, five subgroups, numerous grouplets, closely related, mainly formed by crystal segregation in rapidly cooling melts. *Geochim. Cosmochim. Acta* **66**, 2445–2473.

Wasson, J.T., Lange, D.E., Francis, C.A., Ulff-Møller, F., 1999. Massive chromite in the Brenham pallasite and the fractionation of Cr during the crystallization of asteroidal cores. *Geochim. Cosmochim. Acta* **63**, 1219–1232.

Wasson, J.T., Matsunami, Y., Rubin, A.E., 2006. Silica and pyroxene in IVA irons; possible formation of the IVA asteroid by impact melting and reduction of L-LL-chondrite materials followed by crystallization and cooling. *Geochim. Cosmochim. Acta* **70** (in review).

Wasson, J.T., Ouyang, X., Wang, J., Jerde, E., 1989. Chemical classification of iron meteorites: XI. Multi-element studies of 38 new irons and the high abundance of ungrouped irons from Antarctica. *Geochim. Cosmochim. Acta* **53**, 735–744.

Wasson, J.T., Richardson, J.W., 2001. Fractionation trends among IVA iron meteorites: contrasts with IIIAB trends. *Geochim. Cosmochim. Acta* **65**, 951–970.